SNX17 protects integrins from degradation by sorting between lysosomal and recycling pathways

Florian Steinberg,[1] Kate J. Heesom,[2] Mark D. Bass,[1] and Peter J. Cullen[1]

[1]The Henry Wellcome Integrated Signalling Laboratories and [2]Proteomics Facility, School of Biochemistry, School of Medical Sciences, University of Bristol, Bristol BS8 1TD, England, UK

The FERM-like domain–containing sorting nexins of the SNX17/SNX27/SNX31 family have been proposed to mediate retrieval of transmembrane proteins from the lysosomal pathway. In this paper, we describe a stable isotope labeling with amino acids in culture–based quantitative proteomic approach that allows an unbiased, global identification of transmembrane cargoes that are rescued from lysosomal degradation by SNX17. This screen revealed that several integrins required SNX17 for their stability, as depletion of SNX17 led to a loss of β1 and β5 integrins and associated α subunits from HeLa cells as a result of increased lysosomal degradation. SNX17 bound to the membrane distal NPXY motif in β integrin cytoplasmic tails, thereby preventing lysosomal degradation of β integrins and their associated α subunits. Furthermore, SNX17-dependent retrieval of integrins did not depend on the retromer complex. Consistent with an effect on integrin recycling, depletion of SNX17 also caused alterations in cell migration. Our data provide mechanistic insight into the retrieval of internalized integrins from the lysosomal degradation pathway, a prerequisite for subsequent recycling of these matrix receptors.

Introduction

During cell migration, many membrane proteins undergo endocytosis (Caswell et al., 2009; Bass et al., 2011) and enter the endosomal network, where sorting mechanisms determine their fate. Initially, cargo proteins pass through the early endosome, where they are segregated between entry into the lysosomal pathway, leading to degradation, or recycling back to the plasma membrane or into the biosynthetic pathway (Johannes and Popoff, 2008; Grant and Donaldson, 2009). Sorting nexins are phosphoinositide-binding proteins that reside preferentially on early endosomes, where they are involved in diverse sorting processes (Worby and Dixon, 2002; Carlton et al., 2005; Seet and Hong, 2006; Cullen, 2008). SNX17 (sorting nexin-17) and SNX27 (sorting nexin-27) have both been shown to mediate cargo retrieval away from the degradative pathway by association with specific sequences within the cytoplasmic domains of target receptors (van Kerkhof et al., 2005; Lauffer et al., 2010). Here, we describe the development of a novel assay based on quantitative proteomics to allow an unbiased global identification of the key transmembrane proteins that are retrieved from degradation by SNX17. This revealed that depletion of SNX17 in HeLa cells resulted in lysosomal degradation of multiple members of the integrin family of extracellular matrix receptors. We show that retrieval of integrins from the lysosomal pathway was caused by an interaction between the membrane-distal NPXY motif of integrin β subunits and a noncanonical FERM domain within SNX17. Consistent with enhanced degradation, we present evidence that integrin recycling and cell surface expression is severely impaired in SNX17-depleted cells, resulting in changes in cell migration.

Results and discussion

To establish a global view of cargo proteins that use SNX17 for retrieval from the degradative pathway, we developed a novel, unbiased method for the identification of transmembrane proteins that are specifically lost upon SNX17 RNAi-mediated suppression. Because depletion of SNX17 results in reduced levels of the LRP1 (low density lipoprotein receptor–related protein 1; van Kerkhof et al., 2005), we reasoned that other SNX17 cargo molecules should also display decreased

Correspondence to Peter J. Cullen: Pete.Cullen@bristol.ac.uk

Abbreviations used in this paper: MEF, murine embryonic fibroblast; MS, mass spectrometry; SILAC, stable isotope labeling with amino acids in culture; WASH, Wiskott–Aldrich syndrome protein and scar homolog.

The Rockefeller University Press $30.00
J. Cell Biol. Vol. 197 No. 2 219–230
www.jcb.org/cgi/doi/10.1083/jcb.201111121

A

SNX27	SNX17		
Score	Light/Heavy	Light/Medium	detected protein
12.31	1.078	13.990	Phosphate carrier protein, mitochondrial (SLC25A3)
16.85	1.922	10.928	SLIT and NTRK-like protein 4 (SLITRK4)
18.58	0.727	10.759	Transmembrane protein 214 (TMEM214)
10.93	1.873	8.122	Lysosomal acid phosphatase (ACP2)
64.62	2.139	5.567	Integrin α-5 (ITGA5)
163.94	1.180	4.810	Integrin β-1 (ITGB1)
10.44	1.321	4.288	Neuropilin-1 (NRP1)
26.47	0.921	4.131	Roundabout homologue 1 (ROBO1)
122.48	1.481	4.079	Prolow-density lipoprotein receptor-related protein 1 (LRP1)
26.72	1.468	3.101	Chloride intracellular channel protein 4 (CLIC4)
61.08	1.832	3.083	Solute carrier family 12 member 4 (SLC12A4)
157.90	1.300	3.051	Large neutral amino acids transporter small subunit 1 (SLC7A5)
61.47	1.122	3.046	Integrin α-3 (ITGA3)
107.42	1.659	2.998	Integrin α-6 (ITGA6)
20.10	1.457	2.997	Tyrosine-protein kinase transmembrane receptor ROR2 (ROR2)

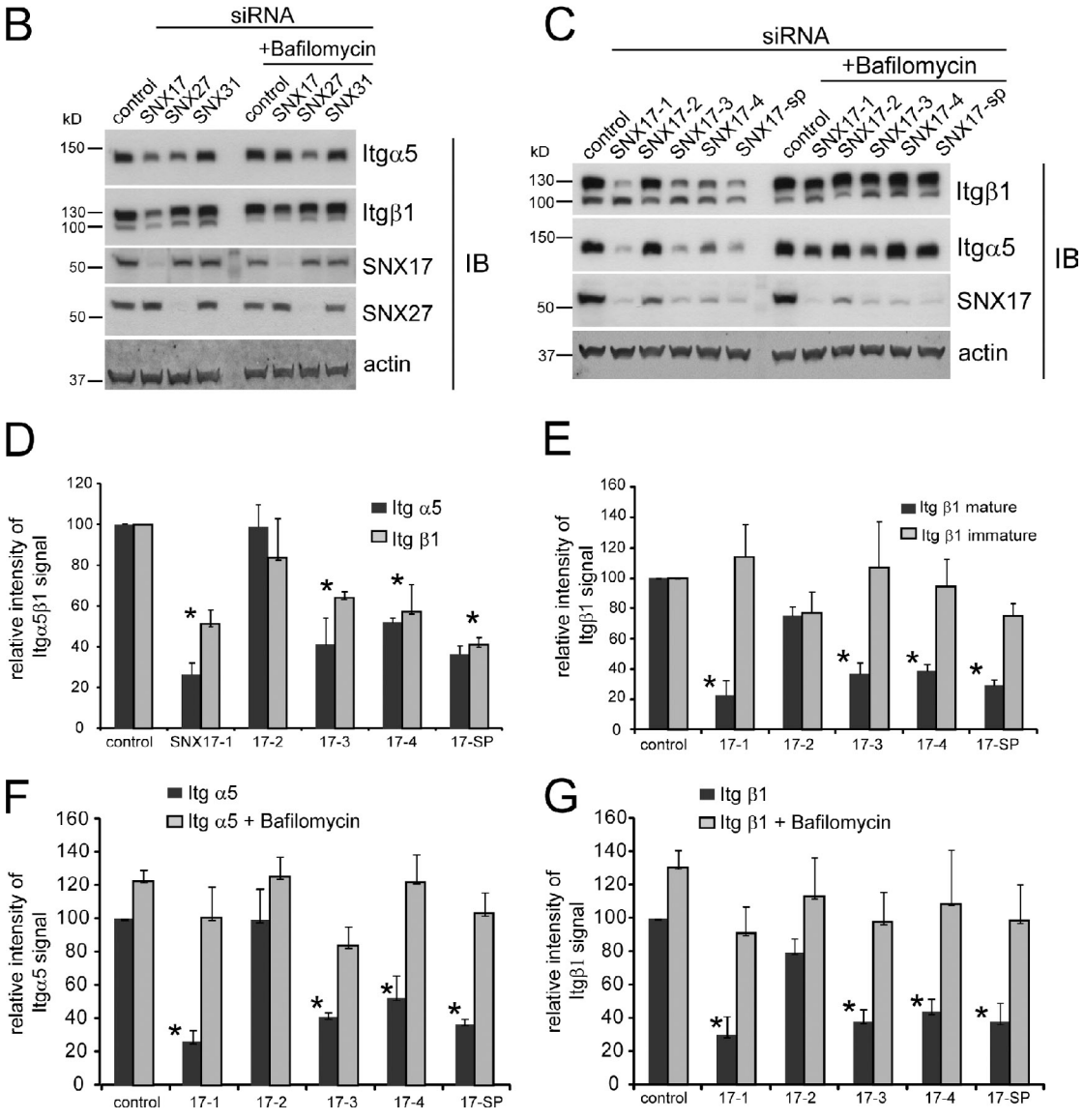

Figure 1. **Proteomic identification of integrin receptors as cargoes for SNX17.** (A) The table lists transmembrane proteins that were at least threefold less abundant in SNX17-depleted HeLa cells compared with control. The light/medium is the ratio between the abundance of the respective protein in control cells compared with SNX17-depleted cells. Light/heavy is the ratio between the detected proteins in control versus SNX27-suppressed cells. (B) Overnight

protein levels upon RNAi-mediated suppression of this sorting nexin. We used stable isotope labeling with amino acids in culture (SILAC) to compare the abundance of membrane proteins between SNX17-depleted and control HeLa cells. To ensure identification of SNX17-specific cargos, we compared SNX17-depleted and control extracts with extracts of SNX27-depleted cells. HeLa cells were cultured in media containing light (control), medium (SNX17), and heavy (SNX27) amino acids for 2 wk. Treatment with siRNA efficiently reduced the expression of SNX17 and SNX27 (Fig. S1 A). A crude membrane extract was prepared from the cells, and the relative abundance of membrane proteins was analyzed by quantitative mass spectrometry (MS). The table in Fig. 1 A lists all membrane proteins that suffered a reduction in abundance of threefold or greater in SNX17-depleted cells but were not grossly altered in SNX27-depleted extracts. Importantly, we detected a pronounced loss of LRP1 specifically in the SNX17-depleted cells, which supported the validity of our proteomics approach. Surprisingly, several integrin receptors, most notably Itgα5 (integrin α5) and Itgβ1 (integrin β1), appeared to be present at much lower levels in the SNX17-depleted extracts. Itgα6 (integrin α6) and Itgα3 (integrin α3) were also among the proteins that were detected at much lower levels in SNX17-depleted cells (Fig. S1 B lists all detected integrins and their SILAC ratios).

To test whether integrins were lost because of enhanced lysosomal degradation, we analyzed the level of Itgα5β1 in SNX17- and SNX27-depleted cells treated with and without bafilomycin A, which blocks lysosomal degradation by inhibiting endosomal acidification (Huss and Wieczorek, 2009). In confirmation of the proteomics data, we detected a pronounced loss of Itgβ1 in SNX17-depleted cells (Fig. 1 B). As indicated by our proteomics data, Itgα5 was lost from SNX17-depleted cells but also from cells treated with SNX27 siRNA. However, bafilomycin rescued only the effect of SNX17 depletion on Itgα5 and Itgβ1 levels (Fig. 1 B), whereas the loss of Itgα5 in SNX27-depleted cells was not affected by bafilomycin treatment, suggesting alterations at the transcriptional level. Because of this, we did not further investigate the relationship between SNX27 and Itgα5. Further RNAi experiments with four different siRNA oligonucleotides (oligos) against SNX17 confirmed the loss of Itgα5β1 under SNX17-suppressed conditions (Fig. 1 C), which could be reversed by bafilomycin treatment for all individual oligos. Quantitative PCR confirmed that the loss of Itgα5β1 in SNX17-depleted cells was not caused by transcriptional down-regulation (Fig. S1 C). Quantification of integrin protein levels revealed that <80% of Itgα5 and <60% of total Itgβ1 were lost from SNX17-depleted cells and could be rescued by bafilomycin treatment (Figs. 1 D and S1 D). We saw a clear correlation between the levels of SNX17 suppression (Fig. S1 E) and the corresponding loss of Itgα5β1 (R^2 value of 0.61; Fig. S1 F). In HeLa and other cell lines, Itgβ1 exists in an immature Golgi resident form of ∼100 kD, which is not yet glycosylated, and a mature form of 130 kD (Salicioni et al., 2004). If SNX17 mediates endosomal recycling of Itgβ1, depletion of SNX17 should not affect the newly synthesized immature form but only the mature form, which is subject to recycling. Knockdown with the three most efficient individual oligos (17-1, 17-3, and 17-4) did not lead to a loss of the immature form of Itgβ1 (Fig. 1 E), whereas <80% of the mature form was lost with the most effective siRNA. In these experiments, overnight treatment (18 h) of the cells with bafilomycin restored Itgα5β1 levels to control levels (Fig. 1, F and G). The effect of SNX17 depletion was also manifested by a change in surface expression, as assessed by flow cytometry. SNX17-depleted cells had drastically reduced levels of active and inactive Itgβ1 as well as Itgα5 at the cell surface (Fig. 2). An analysis of other integrin receptors showed that surface expression of Itgα3 and Itgα6, both of which appeared as potential hits in our initial proteomic screen (Fig. 1 A), was reduced. ItgαV and Itgβ5 surface levels were also affected by depletion of SNX17, although the loss was more variable and not as pronounced as the loss of most of the β1 integrins (Fig. 2). To further confirm that depletion of SNX17 decreases integrin stability, we performed degradation assays in cells treated with cycloheximide to block protein synthesis. Consistent with previously published data (Lobert et al., 2010), Itgα5β1 was stable over the course of 7 h in control cells, in which integrin is recycled rather than degraded (Fig. 3 A). In contrast, Itgα5β1 stability was dramatically decreased in SNX17-depleted cells. Biochemical internalization and recycling assays revealed that although Itgα5β1 was internalized at similar relative rates in SNX17-depleted cells (Fig. 3 B), the return to the cell surface was severely inhibited (Fig. 3 C). To identify the endosomal compartment where integrin recycling stalled in SNX17-depleted cells, we performed antibody-based recycling assays. Although internalized antibody against inactive (Fig. 3 D) and active Itgβ1 (Fig. S1 G) efficiently returned to the cell surface within 30 min in control cells, almost no antibody was recycled back to the surface in SNX17-depleted cells. Instead, internalized antibody accumulated in internal vesicles, which were absent in control cells (Figs. 3 D and S1 E). An endosomal marker analysis revealed that the majority of these vesicles were EEA1- and Rab4-positive recycling endosomes, whereas some were already Rab7- or LAMP1-decorated late endosomes/lysosomes (Fig. 3 E). No Rab5 and little Rab11 were detected on the vesicles. When lysosomal proteolysis was blocked by bafilomycin in SNX17-depleted cells overnight, a staining of Itgβ1 and LAMP1 showed that most of the integrin had accumulated in lysosomes (Fig. 3 F). Collectively, the data

treatment with 100 nM bafilomycin A prevents loss of integrins in SNX17- and SNX27-depleted cells. (C) Western blot showing the effect of four different SNX17 siRNAs and a pool (SMARTpool [sp]) of these four oligos on Itgα5/β1 levels and the effect of bafilomycin treatment. (D) Quantitative Western blot analysis of the effect of SNX17 suppression on total Itgα5 and β1 levels. The graph represents the mean of five independent experiments. (E) Quantitative analysis of the effect of SNX17 suppression on the mature (130 kD) and the immature (100 kD) forms of Itgβ1. The graph represents the mean of three independent experiments. (F and G) Bafilomycin rescue of the loss of Itgα5β1 in SNX17-depleted cells. The graphs show the mean of four independent experiments. *, P < 0.05. IB, immunoblot. Error bars indicate the standard deviation.

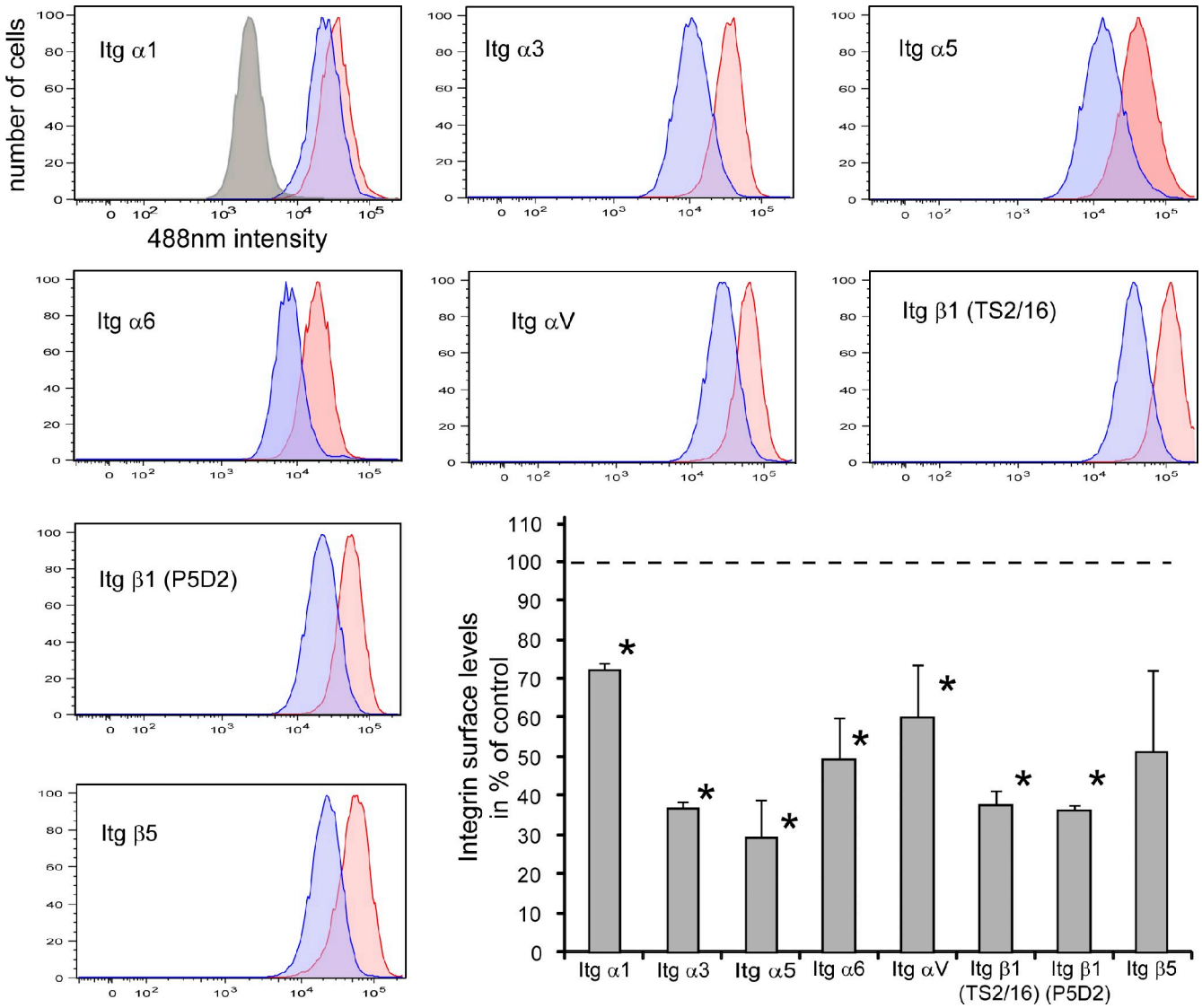

Figure 2. **Flow cytometric analysis of surface integrins in SNX17-depleted HeLa cells.** The histograms show levels of indicated integrins in control (red) and SNX17-depleted cells (blue) including an isotype control (gray). The graph represents the mean fluorescence in at least three independent experiments in the percentage of control levels. The dotted line represents the control level, set to 100% for each integrin. The error bars represent the standard deviation. *, $P < 0.05$.

suggested that in SNX17-depleted cells, Itgβ1 recycling stalls in EEA1/Rab4-positive recycling endosomes followed by aberrant missorting into lysosomes.

Consistent with a role of SNX17 in recycling from early or sorting endosomes, SNX17-GFP colocalized almost completely with EEA1 but could not be detected on LAMP1-positive lysosomes (Fig. S2 A). In antibody uptake assays, internalized Itgβ1 colocalized with SNX17-GFP on EEA1-positive endosomes as early as 2.5 min after internalization (Figs. 4 A and S2 A). This was independent of the activity state of Itgβ1, as we observed strong colocalization with total (K20), active (TS2/16), and inactive (P5D2) Itgβ1 (Fig. S3 A). Immunoprecipitation of endogenous Itgβ1 coprecipitated endogenous SNX17, although the signal was only barely above background, indicating low stoichiometry and/or affinity between SNX17 and the integrin (Fig. 4 B). However, a GFP-Trap immunoprecipitation of full-length Itgβ1-GFP, stably expressed in Itgβ1$^{-/-}$ murine embryonic fibroblasts (MEFs), clearly revealed an association of endogenous SNX17 with Itgβ1 (Fig. 4 C). When overexpressed in HEK293 cells, the isolated cytoplasmic tail of Itgβ1 fused to an N-terminal GFP tag efficiently precipitated endogenous SNX17. In contrast, the cytoplasmic tails of Itgα5 or ItgαV failed to coprecipitate SNX17, suggesting that SNX17 binds the β subunit of the integrin heterodimer (Fig. 4 D). In support of this, SNX17 also coprecipitated with the isolated Itgβ5 cytodomain (Fig. 4 E), demonstrating that SNX17 retrieves integrin heterodimers from degradation by targeting the β subunit. As SNX17 contains a C-terminal noncanonical FERM-like domain that engages cargo by binding to tyrosine-based motifs (Stockinger et al., 2002; Burden et al., 2004; van Kerkhof et al., 2005; Ghai et al., 2011), we tested whether SNX17 binds to the β integrin NPXY motifs by substituting the critical tyrosine residues within the two NPXY motifs in the Itgβ1 and β5 cytoplasmic tail. Indeed, mutation of the membrane-distal

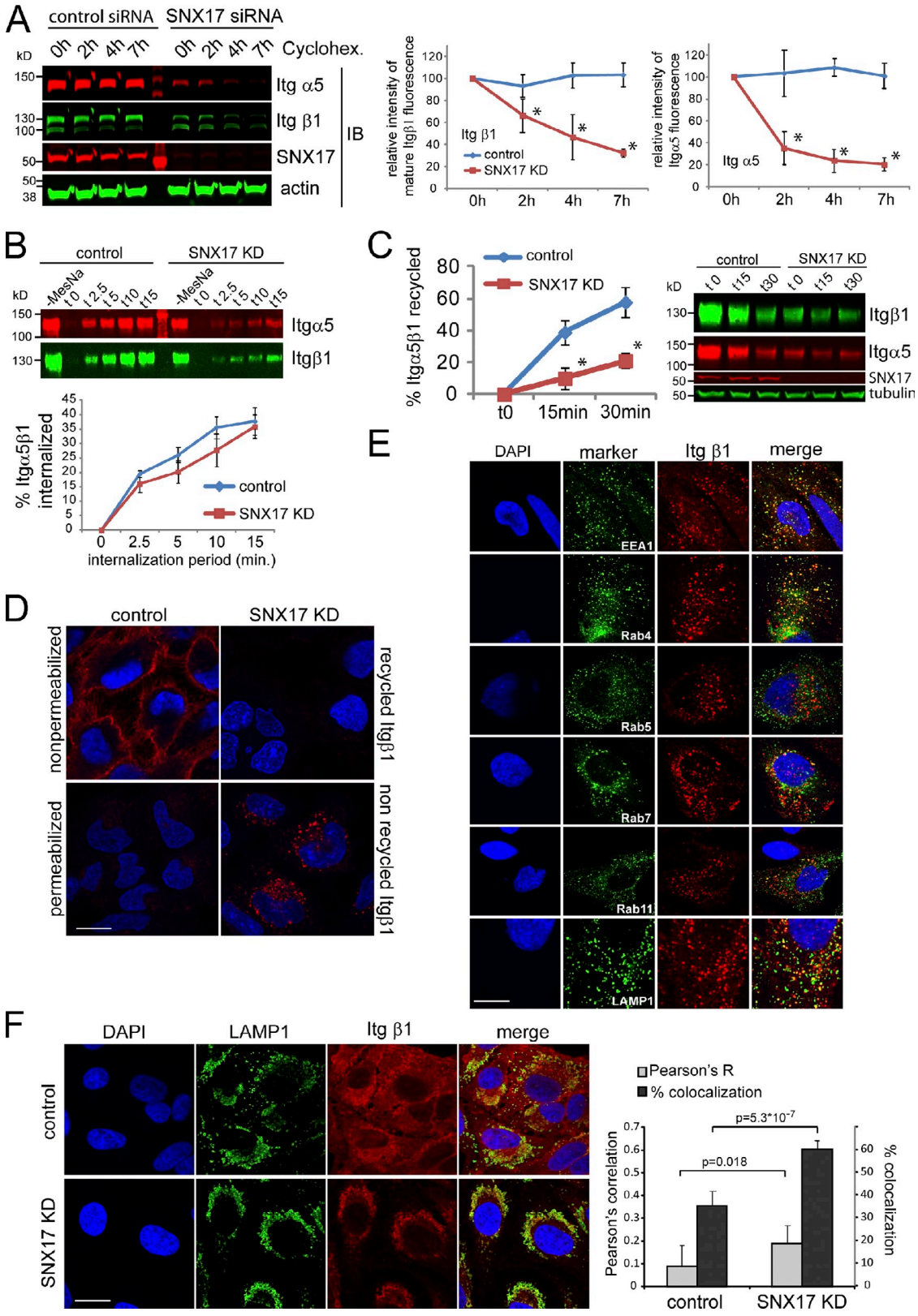

Figure 3. **SNX17 depletion decreases Itgα5β1 recycling and leads to enhanced degradation of integrins caused by aberrant trafficking to lysosomes.** (A) Itgα5β1 levels in control and SNX17-depleted HeLa cells treated with cycloheximide (Cyclohex.) over the indicated periods. Error bars indicate the standard deviation of three experiments. (B) Biochemical internalization assay of Itgα5β1 in control and SNX17-depleted cells. (C) Biotinylation-based recycling assay of Itgα5β1 in SNX17-depleted HeLa cells. The blot shows a representative experiment. (B and C) Error bars represent the SEM of four experiments. (D) Recycling assay with antibody against inactive (P5D2) Itgβ1. (E) Endosomal marker analysis of inactive Itgβ1 in vesicles remaining within the SNX17-depleted cells after a 30-min chase period. (F) Colocalization analysis of Itgβ1 and the lysosomal marker LAMP1 in control and SNX17-depleted cells treated with bafilomycin for 14 h. The Pearson's correlation and the percentage of colocalization are based on eight images from two independent experiments. The error bars represent the standard deviation. Bars, 10 µm. IB, immunoblot; KD, knockdown.

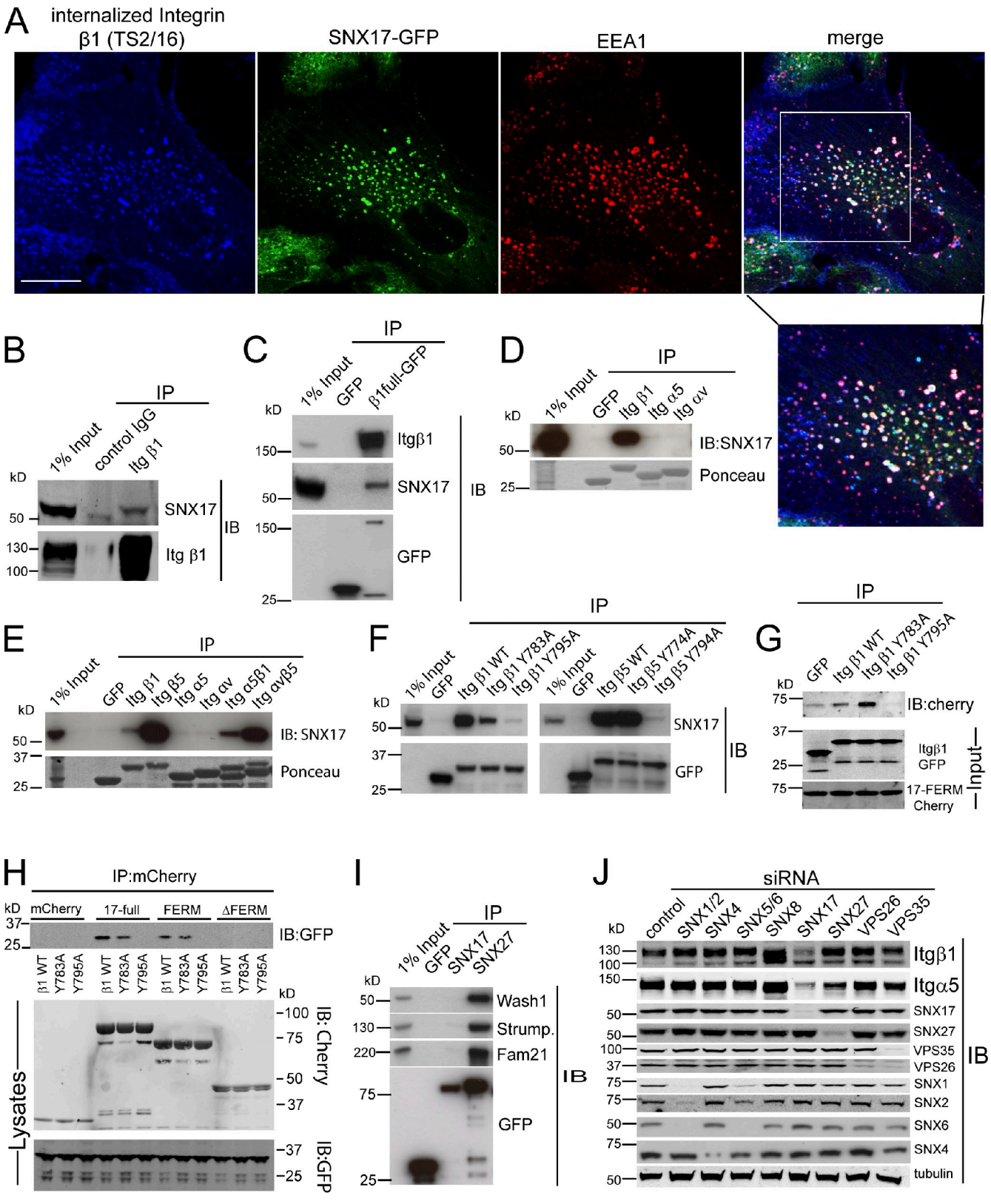

Figure 4. **SNX17 binds to the membrane-distal NPXY motifs in β integrins.** (A) Confocal image of internalized antibody (TS2/16) against active Itgβ1, endogenous EEA1, and GFP-tagged SNX17 in human RPE1 cells after 30 min of internalization. The boxed area is magnified below the merged image. Bar, 20 µm. (B) Western blot analysis of SNX17 in an immunoprecipitation of endogenous Itgβ1. (C) GFP-Trap precipitation of retrovirally expressed full-length Itgβ1-GFP from Itgβ1$^{-/-}$ MEFs and Western blot analysis of endogenous SNX17 in the precipitates. The GFP blot shows expression of Itgβ1-GFP and GFP. (D) GFP-Trap precipitations of transiently transfected GFP-tagged cytoplasmic tails of indicated integrins from HEK293 cells. The blot shows endogenous SNX17 that precipitated with the Itgβ1 cytoplasmic tail. (E) Blot showing endogenous SNX17 in GFP-Trap precipitations of GFP-tagged integrin cytoplasmic tails. (F) GFP-Trap precipitations of Y motif mutated Itgβ1 and β5 cytoplasmic tails. (G) GFP-Trap precipitation of in vitro translated Itgβ1

NPXY motif blocked coprecipitation of SNX17 with the GFP-tagged Itgβ1 and β5 cytoplasmic tail (Fig. 4 F). In vitro translated wild-type and Y783A, but not the Y795A, cytoplasmic domain also precipitated the in vitro translated mCherry-tagged SNX17-FERM domain (Fig. 4 G), indicating direct binding. Conversely, mCherry-tagged SNX17 and the mCherry-tagged FERM-like domain, but not the ΔFERM protein, precipitated the wild-type and Y783A-mutated Itgβ1 cytoplasmic tail but not the Y795A protein (Fig. 4 H). Collectively, these data demonstrate that SNX17 retrieves integrins from the lysosomal degradative pathway by binding of its FERM-like domain to the membrane-distal NPXY motif of the β subunit. As the distal NPXY motif is also the binding site for the focal adhesion–associated Kindlin proteins (Moser et al., 2009), both proteins could compete for this site. However, we did not detect Kindlin-2 on SNX17-GFP–labeled endosomes that contained Itgβ1 (Fig. S3 B), suggesting that these proteins function in spatially segregated compartments.

SNX17 is closely related to SNX27 (Ghai et al., 2011), which binds indirectly to the retromer complex via the actin nucleation–promoting Wiskott–Aldrich syndrome protein and scar homolog (WASH) complex (Temkin et al., 2011) that has recently also been shown to be required for Itgα5β1 recycling (Zech et al., 2011). Moreover, there are existing links between SNX17 and the retromer complex, as both have been shown to be involved in the trafficking of the Alzheimer's-related APP protein (Lee et al., 2008; Muhammad et al., 2008; Lane et al., 2010). This caused us to ask whether SNX17 also links cargo recognition of the integrin NPXY motifs to retromer carrier formation through an association with the WASH complex. SNX17 did not precipitate members of the WASH complex, whereas SNX27 efficiently precipitated the WASH complex components WASH1, FAM21, and Strumpellin (Fig. 4 I; Gomez and Billadeau, 2009). Moreover, depletion of the retromer subunits VPS26 or VPS35 as well as suppression of retromer-associated sorting nexins, SNX1, SNX2, SNX5, and SNX6 (Wassmer et al., 2007, 2009), did not result in a loss of Itgα5β1 (Fig. 4 J), indicating that retrieval of integrins does not rely on SNX17 engaging the retromer complex.

As SNX17 rescues integrins from lysosomal degradation by binding to the membrane-distal tyrosine motif, we next asked whether mutation of Y795 in Itgβ1 would phenocopy the effect of SNX17 depletion. Y783 and Y795 in full-length human Itgβ1 were mutated to alanine and the respective constructs were lentivirally expressed in immortalized Itgβ1$^{-/-}$ MEFs. Strikingly, the Y795A, but not the Y783A, mutation led to a dramatic change in subcellular localization, as most of the inactive (Fig. 5 A) and active (Fig. S3 C) Itgβ1-Y795A accumulated in LAMP1-positive lysosomes. In agreement with the observed mislocalization to lysosomes, degradation assays revealed that the mature form of Itgβ1-Y795A mutant was quickly degraded, whereas wild type and the Y783A mutant were stable over 7 h. Furthermore, treatment with bafilomycin restored the mature 130-kD band of the Y795A mutated integrin (Fig. 5 C).

Finally, we asked whether SNX17 depletion affected focal adhesion formation and migration. Depletion of SNX17 in fibroblasts led to an almost complete loss of mature Itgβ1 and to a 70% loss of Itgα5 but only to a slight reduction in ItgαV levels (Fig. 5 D). The fall in integrin levels caused a reduction in total focal adhesion area and mean adhesion size in fibroblasts spread on fibronectin (Fig. 5 E). When migration through a fibrillar cell-derived matrix was analyzed, SNX17-depleted fibroblasts and HeLa cells both demonstrated increased directional persistence and increased speed (Figs. 5 F and S3 D and Video 1). Changes in speed and persistence are consistent with a shift from Itgα5β1-mediated to ItgαVβ3-mediated adhesion. Antibody inhibition of Itgα5β1 has been shown to increase persistence of migration as the cell relies on ItgαVβ3 (White et al., 2007). Furthermore, large Itgα5β1-rich adhesions have been found to act as static structures, whereas small ItgαVβ3-rich adhesions promote cell migration (Roca-Cusachs et al., 2009), meaning that reduction of adhesion area and Itgα5β1 levels would both contribute to fast, persistent migration.

Collectively, the data presented herein have established that our novel proteomic approach is a useful tool for the global identification of transmembrane cargos of endosomal sorting adaptors. In the context of SNX17, it allowed an unbiased identification of several integrins as cargo molecules for this sorting nexin. This approach could therefore be used to identify novel cargo for other endosomal sorting complexes, such as the retromer complexes (Arighi et al., 2004; Carlton et al., 2004; Seaman, 2004; Wassmer et al., 2007, 2009; Harterink et al., 2011; Cullen and Korswagen, 2012), further sorting nexins, or other endosomal proteins that are involved in the retrieval of cargo away from the lysosomal pathway. Our data have established that SNX17 is required for the efficient recycling of Itgα5β1 from an EEA1/Rab4-positive compartment, where direct binding of SNX17 to the membrane-distal NPXY motif prevents an entry into the degradative pathway. With regard to the mechanistic basis of SNX17-mediated lysosomal retrieval, it appears that SNX17, unlike its family member SNX27, is not an adaptor for the retromer complex. To our knowledge, SNX17 is the first integrin-associated protein whose loss results in the lysosomal degradation of integrins. Although several other proteins, including ACAP1 (Li et al., 2005) and EHD1 (Jović et al., 2007), have been shown to be required for integrin recycling (Margadant, et al., 2011), all of these recycling processes take place at a later stage in the endosomal network. Hence, loss of function of these proteins causes an accumulation of Itgβ1 in intracellular vesicles but no overall loss of these receptors. A recent study found enhanced lysosomal degradation of Itgβ1 when syntaxin 6 function was disrupted (Tiwari et al., 2011); however, this is probably

cytoplasmic tails with Y motif mutations and the in vitro translated mCherry-tagged SNX17-FERM domain. (H) RFP-Trap precipitations of mCherry-tagged SNX17 domains and GFP-tagged Itgβ1 cytoplasmic tails with Y motif mutations. (I) GFP-Trap precipitation of SNX17 and SNX27 and Western blot analysis of WASH components. (J) Analysis of Itgα5β1 levels in a HeLa cell with suppressed expression of indicated sorting nexins and retromer components. IP, immunoprecipitation; IB, immunoblot; Strump., Strumpellin.

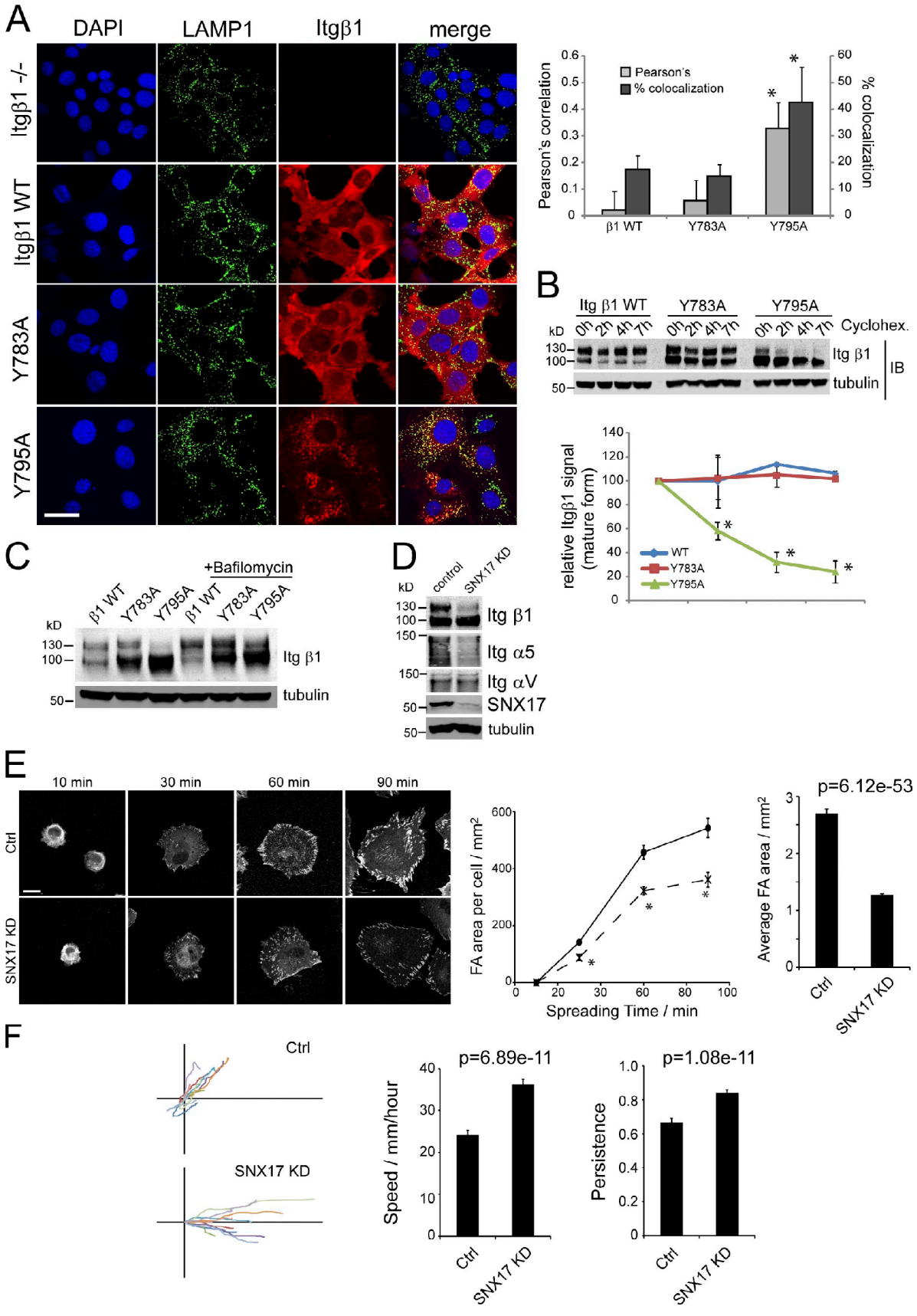

Figure 5. **Analysis of Y mutation in the tail of Itgβ1 and effects of SNX17 depletion on cell migration.** (A) Immunofluorescent staining and quantitative colocalization analysis of endogenous LAMP1 and lentivirally expressed Itgβ1 with the indicated mutations in Itgβ1$^{-/-}$ MEFs. Error bars represent the standard deviation of twelve images from two experiments. (B) Degradation assay of the Itgβ1 proteins under cycloheximide (Cyclohex.)-treated conditions.

not specific for a class of cargo, as a loss of endosomal SNARE function will most likely perturb endosomal function in general. Collectively, our data establish that the membrane-distal NPXY motif of Itgβ1 and possibly other β integrins serves as a lysosomal avoidance signal by engaging the FERM-like domain of SNX17 on early endosomes, thereby enabling entry into recycling pathways further downstream.

Materials and methods

Tissue culture
HeLa and RPE1 cells were cultured in DME under standard conditions. Human fibroblasts were cultured in DME supplemented with 15% FBS, 4.5 g/liter glucose, 25 mM Hepes, and 2 mM L-glutamine. Immortalized Itgβ1$^{-/-}$ MEF cells were cultured at 33°C in DME supplemented with 10% FBS and interferon λ. For the SILAC experiments, HeLa cells were cultured in control, R6K4, and R10K8 DME medium (Dundee Cell Products) supplemented with 10% dialyzed FBS (Dundee Cell Products).

Viral expression of GFP-tagged Rab proteins and human Itgβ1
The human Itgβ1 cDNA clone was obtained from OriGene and subcloned into pcDNA 3.1 using a primer for the wild-type protein as well as one with the Y795A mutation. The Y783A mutation was introduced into the wild-type sequence with site-directed mutagenesis. From pcDNA3.1, the Itgβ1 sequence was transferred into the pXLG3 lentiviral expression plasmid, and lentivirus was produced in HEK293 cells. The Itgβ1$^{-/-}$ MEFs were cultured in the HEK293-conditioned media containing the respective viruses for 4 d. For Rab-GFP expression, HeLa cells were exposed to lentivirus expressing the respective rab proteins at low levels for 3 d followed by culturing for 1 wk before further experiments.

SILAC experiments
HeLa cells were cultured in 6-well plates for 2 wk in R0K0 control, R6K4, and R6K10 media supplemented with 10% dialyzed FBS (media and FBS were obtained from Dundee Cell Products). 200,000 cells per well of a 6-well plate were reverse transfected with scrambled (R0K0), SNX17 (R6K4), and SNX27 (R10K8) siRNA oligos (ON-TARGETplus SMARTpool; Thermo Fisher Scientific) with reagent (HiPerFect; QIAGEN) according to the manufacturer's reverse transfection protocol. 14 h after the first transfection, cells were transfected again using the manufacturer's standard protocol. The cells were then incubated another 60 h. For the liquid chromatography–MS analysis of membrane proteins, the cells were detached from the culture dishes with 5 mM EDTA in PBS for 20 min. To verify the efficacy of the siRNA treatment, a fraction of the cells was lysed in standard lysis buffer and subjected to control Western blotting of SNX17 and SNX27. From the remaining cells, a crude membrane extract was obtained with a subcellular fractionation kit (QProteome; QIAGEN). The resulting membrane fractions were resolved on precast PAGE gels (NuPAGE 4–12%; Invitrogen) stained with colloidal Coomassie (SimplyBlue SafeStain; Invitrogen) followed by quantification of the amount of protein with a scanner (Odyssey; LI-COR Biosciences). The samples were then pooled in ratios according to the protein quantification, resolved by SDS-PAGE, stained with colloidal Coomassie, and analyzed by liquid chromatography–MS/MS-based quantification. For that, the lane was subjected to "gel walking" and cut into 10 slices, all of which were subsequently subjected to in-gel tryptic digestion using an automated digestion unit (ProGest; Digilab UK). The resulting peptides were fractionated using a nano-HPLC system (UltiMate 3000; Dionex). In brief, peptides in 1% (vol/vol) formic acid were injected onto a C18 nanotrap column (Acclaim PepMap; Dionex). After washing with 0.5% (vol/vol) acetonitrile, 0.1% (vol/vol) formic acid peptides were resolved on a 250 mm × 75–µm C18 reverse-phase analytical column (Acclaim PepMap) over a 120-min organic gradient with a flow rate of 300 nl/min^{-1}. Peptides were ionized by nanoelectrospray ionization at 2.3 kV using a stainless steel emitter with an internal diameter of 30 µm (ES542; Proxeon). Tandem MS analysis was performed on a mass spectrometer (LTQ Orbitrap Velos; Thermo Fisher Scientific). The Orbitrap was set to analyze the survey scans at 60,000 resolution, and the top six ions in each duty cycle were selected for MS/MS in the LTQ linear ion trap. Data were acquired using the Xcalibar v2.1 software (Thermo Fisher Scientific). The raw data files were processed and quantified using Proteome Discoverer software v1.2 (Thermo Fisher Scientific) with searches performed against the UniProt human database by using the SEQUEST algorithm with the following criteria: peptide tolerance at 10 ppm, trypsin as the enzyme, and carboxyamidomethylation of cysteine as a fixed modification. The reverse database search option was enabled, and all data were filtered to satisfy a false discovery rate of <5%.

siRNA transfections
For all siRNA-based experiments, a scrambled siRNA SMARTpool was used for the control cells. ON-TARGET SMARTpools, which are a mixture of four different oligos, were used to suppress SNX17 and SNX27 (Wassmer et al., 2007). For SNX17, the four oligos comprising the SMARTpool reagent were also used individually. HiPerFect or DharmaFECT 1 (Thermo Fisher Scientific) was used for all transfections according to the manufacturer's instructions.

Real-time PCR analysis
HeLa cells were transfected with oligo 17-1 (Thermo Fisher Scientific) and incubated for 72 h followed by TRIZOL (Sigma-Aldrich) extraction of total RNA. cDNA was transcribed using a synthesis kit (RevertAid Premium; Fermentas), and the mRNA abundance of SNX17, Itgα5β1, and glyceraldehyde 3-phosphate dehydrogenase was analyzed on a cycler (Opticon; MJ Research) with SYBR green 2× master mix obtained from Abgene. The intron-spanning primers were designed with the assay design center of the Universal ProbeLibrary (Roche).

Antibodies and other reagents
Bafilomycin A was purchased from Tocris Bioscience, and cycloheximide was obtained from Sigma-Aldrich. The rabbit polyclonal antibody against SNX17 was a gift from G. Bu (Washington University, St. Louis, MO). Monoclonal integrin antibodies for the FACS analysis were K20 against total β1 (Santa Cruz Biotechnology, Inc.), TS2/16 against active β1 (Santa Cruz Biotechnology, Inc. and BioLegend), P5D2 against inactive Itgβ1 (Santa Cruz Biotechnology, Inc.), Itgβ5 (AST-3T; BioLegend), Itgα1 (MAB 1973; Millipore), Itgα3 (MCA1948T; AbD Serotec), Itgα5 (NKI-SAM1; BioLegend), Itgα6 (MCA1457; AbD Serotec), and ItgαV (17E6; EMD). For Western blotting, the following were used: anti-CD29 (610467; BD) for Itgβ1 Western blotting and rabbit polyclonal against Itgα5 (SC-10729; Santa Cruz Biotechnology, Inc.). Mouse monoclonal anti–β-actin and antitubulin were obtained from Sigma-Aldrich. Anti-LAMP1 (rabbit polyclonal; AB24170) as well as anti–Kindlin-2 (AB74030) was purchased from Abcam. Anti-WASH1 and anti-FAM21 were gifts from D.D. Billadeau (Mayo Clinic, Rochester, MN). The rabbit polyclonal antibody against Strumpellin as well as the goat polyclonal antibody against EEA1 was purchased from Santa Cruz Biotechnology, Inc.

Migration analysis
Cell-derived matrices were generated by culturing confluent fibroblasts for 10 d before removing the fibroblasts by NH_4OH lysis. For migration, control or SNX17 knockdown cells were seeded at 5,000 cells/ml and allowed to spread for 4 h before capturing time-lapse images at 10-min intervals for 10 h on a microscope (AS MDW; Leica) using a 5×/0.15 NA Fluotar objective and a charge-coupled device camera (CoolSNAP HQ; Roper Scientific). The migration paths of all nondividing, nonclustered cells were tracked using ImageJ software (National Institutes of Health), and persistence was determined by dividing linear displacement of a cell over 10 h by the total distance migrated.

Flow cytometry
For the detection of surface integrins, HeLa cells were transfected with scrambled and SNX17 siRNA 72 h before harvest of the cells. The cells

Error bars represent the SEM of three experiments. (C) Western blot showing the effect of 14-h bafilomycin treatment on a mature form of mutated Itgβ1. (D) Integrin and SNX17 levels in control and SNX17-depleted fibroblasts. (E) Vinculin-stained fibroblasts spread on fibronectin for 10–90 min and analyzed for total focal adhesion (FA) area per cell (dotted line shows SNX17 knockdown; continuous line shows control cells) and the mean size of individual focal adhesions. (F) Migration tracks and mean speed and persistence values of fibroblasts migrating through a cell-derived matrix. Persistence shows linear displacement/total distance moved. Error bars represent SEM of >60 cells per condition. Bars, 20 µm. *, $P < 10^{-5}$. Blots are representative of three experiments. Ctrl, control; IB, immunoblot; KD, knockdown; WT, wild type.

were detached from the culture dish with 5 mM EDTA in PBS for 20 min, washed once in PBS with 2% vol/vol FBS, resuspended in 30 µl of diluted (1:30 in PBS with 2% vol/vol FBS) primary antibody, and incubated for 30 min on ice. The cells were washed once and incubated with anti–mouse Alexa Fluor 488 secondary antibody (1:50 in PBS with 10% vol/vol FBS) for 20 min. The cells were washed again and resuspended in PBS containing 2% vol/vol FBS and 1% wt/vol PFA. The fluorescence intensity of 20,000 cells for each sample was then analyzed on a flow cytometer (FACSCanto II; BD). A monoclonal antibody against GFP (Roche) served as an isotype control.

Focal adhesion formation

13-mm coverslips were coated with 10 µg/ml fibronectin (Sigma-Aldrich) and blocked with 10 mg/ml BSA. Fibroblasts were plated at a density of 1.25×10^4 cells per coverslip and allowed to spread at 37°C for 10–90 min before fixing with 4% (wt/vol) PFA. Fixed cells were permeabilized with 0.5% (wt/vol) Triton X-100 diluted in PBS and blocked with 3% (wt/vol) BSA in PBS before staining for vinculin (hVin-1; Sigma-Aldrich) and actin (TRITC-phalloidin; Sigma-Aldrich). Focal adhesion area was analyzed by measuring pixel area above an empirically determined threshold of fluorescence intensity using ImageJ software.

Quantitative Western blotting

For the quantification of total integrin and SNX17 levels, the HeLa cells were lysed in PBS with 1% vol/vol Triton X-100 and protease inhibitor cocktail (Roche). The protein content of the samples was determined with Bradford reagent (Bio-Rad Laboratories), and equal amounts were resolved on precast SDS-PAGE gels (NuSep 4–20%) and blotted onto polyvinylidene fluoride membranes (Immobilon-FL; Millipore) followed by detection of Itgα5β1, SNX17, and β-actin levels on the Odyssey system. SNX17 and integrin signal intensity was normalized by the β-actin signal and calculated as a percentage of control for each oligo.

Integrin internalization/recycling assay and endosomal marker analysis

Biotinylation-based internalization and recycling assays were performed as previously described in Dozynkiewicz et al. (2012) (recycling) with Western blot detection of integrins instead of an ELISA assay. In brief, cells were transfected with control and SNX17 siRNA in 12-well plates, split into 6-well plates 14 h after transfection, and incubated for another 48 h. The cells were serum starved for 1 h and washed in ice-cold PBS, and surface proteins were biotinylated with 0.2 mg/ml Sulfo-NHS-SS Biotin (Thermo Fisher Scientific) in cold PBS followed by washing in TBS and placing on ice. The cells were then incubated in prewarmed DME with 10% FBS at 37°C for the indicated time points, whereas control cells remained on ice. Surface biotin was then stripped from the cells with 2 × 10–min incubation in 50 mM MesNa (Sigma-Aldrich) in TBS, pH 8.6, followed by washing and quenching of the MesNa with 20 mM iodoacetamide (Sigma-Aldrich) in TBS for 10 min. The control cells were not subjected to surface reduction to obtain total surface-labeled integrin. After quenching, the cells were lysed in PBS with 1% Triton X-100 including protease inhibitors. Protein concentration of the lysates was determined with the Bradford reagent, and biotinylated proteins were precipitated from equal amounts of total protein with Streptavidin Sepharose (GE Healthcare). After washing, proteins were eluted from the beads by boiling in SDS sample buffer containing 2.5% β-mercaptoethanol followed by quantitative Western blot analysis of Itgα5β1. The percentage of internalized integrin was calculated from the signal intensity of MesNa-resistant (internalized) Itgα5 relative to total Itgα5 for each time point in four independent experiments.

For the recycling assay, the same labeling procedure as for the internalization assay was used. Surface-labeled integrins were then allowed to be internalized for 30 min in DME with 10% FBS at 37°C followed by a first stripping of surface label in the buffers described for the internalization assay. The cells were then washed and returned to 37°C in DME with 10% FBS for the indicated time points to chase internalized integrins back to the cell surface. The cells were then subjected to a second round of surface reduction to remove the biotin from recycled integrins. Cell lysis, capture of biotinylated proteins, and detection were performed as described for the internalization assay. Recycling of Itgα5β1 was calculated from the signal intensity of Itgα5 remaining in the cells after 15 and 30 min relative to the control cells (t0) that had not been brought back to 37°C after surface reduction.

For the antibody-based recycling assay, control and SNX17-transfected HeLa cells were incubated with 5 µg/ml antibody against active (TS2/16) and inactive (P5D2) antibody in DME with 10% FBS for 1 h at 37°C. The cells were then washed in ice-cold PBS, and surface-bound antibody was stripped from the cells with cold PBS, pH 2.5, for 2 × 1 min. After the acid rinse, cells were washed once in PBS and returned to prewarmed DME with 10% FBS for 30 min to chase internalized antibody from the cells. For the analysis of the antibody returned to the surface, cells were washed in ice-cold PBS, fixed in cold 4% PFA for 20 min, blocked with 1% BSA in PBS for 10 min, and incubated with anti–mouse Alexa Fluor 594 for 30 min followed by washing and incubation in 0.1% saponin (Sigma-Aldrich) in PBS with DAPI dye. For the analysis of internal integrin, cells were subjected to a second acid rinse after the 30-min chase period to remove recycled antibody from the surface. Cells were then fixed, permeabilized with 0.1% saponin, and stained with anti–mouse Alexa Fluor 594 and DAPI. For the endosomal marker analysis, the same antibody-based assay was performed with the P5D2 antibody in either wild-type HeLa cells (EEA1 and LAMP1) or in HeLa cells with lentiviral expression of Rab4, Rab5, Rab7, and Rab11-GFP. After the second acid rinse, cells were fixed in cold PFA, permeabilized with 0.1% saponin, blocked with 1% BSA in PBS, and stained with antibodies against EEA1 and LAMP1. Representative images were then taken on a confocal laser-scanning microscope (SP5 AOBS; Leica) attached to an inverted epifluorescence microscope (DMI6000; Leica). All images were subjected to removal of noise with Volocity (PerkinElmer), and where needed, brightness was increased uniformly using Photoshop (Adobe).

Integrin degradation assays

HeLa cells were transfected with scrambled or SNX17 siRNA in 12-well plates and incubated for 72 h, and cycloheximide at 10 µg/ml was added to the cells for the indicated time points. Cells were lysed in PBS with 1% vol/vol Triton X-100, and integrin levels were determined by quantitative Western blotting. β-Actin fluorescence intensity was used to normalize the detected levels of integrins. The untreated control was set to 100%, and the level of detected integrins was calculated as the percentage of untreated control for each time point. The same procedure was used for the Itgβ1 degradation assay in the $Itg\beta1^{-/-}$ MEFs with lentiviral reexpression of human Itgβ1 constructs.

Antibody uptake and colocalization assay

Human retinal pigment epithelium (RPE1) cells were transduced with a lentivirus expressing GFP-SNX17. The cells were incubated with a monoclonal antibody against active Itgβ1 at 2 µg/ml for 1.5 h, fixed, permeabilized, and stained with DAPI and an Alexa Fluor 488–coupled secondary antibody against mouse IgG. Image analysis was then performed with the aforementioned laser-scanning microscope (SP5 AOBS).

LAMP1 and Itgβ1 colocalization assay

HeLa cells were transfected with scrambled and SNX17 siRNA and incubated for 60 h. The cells were then treated with 100 nM bafilomycin A for 14 h, fixed, permeabilized with 0.1% saponin, and stained for Itgβ1 (TS2/16) and LAMP1. Colocalization analysis was performed on the confocal section showing maximum LAMP1 signal using Volocity image analysis software. Thresholds were generated with the Volocity auto threshold function. Pearson's correlation as well as the percentage of colocalization of integrin and LAMP1 signal was calculated from eight images taken from two independent experiments.

Immunoprecipitation experiments

Endogenous Itgβ1 was precipitated from HeLa cell extracts (two 150-mm dishes in 1 ml of 50-mM Tris-HCL with 0.5% vol/vol NP-40 and protease inhibitor cocktail) with 10 µg antibody (TS2/16 or anti-GFP as a control antibody) and protein G–agarose under shaking for 3 h at 4°C. The precipitates were analyzed for the presence of endogenous SNX17 by Western blotting. The isolated cytoplasmic tails of the respective integrins were cloned from HeLa cDNA and ligated into pEGFP-C1. Site-directed mutagenesis was used to change the indicated tyrosine residues into alanines. The constructs were overexpressed in HEK293 cells using polyethyleneimine (Sigma-Aldrich). 48 h after transfection, cells were lysed in 1 ml of 50-mM Tris-HCL, pH 7.8, with 0.5% vol/vol NP-40 and protease inhibitor cocktail. The cytoplasmic tails were then precipitated with GFP-Trap beads (Chromotek) for 30 min followed by Western blot analysis of endogenous SNX17 in the precipitates. Full-length Itgβ1-GFP was retrovirally expressed in $Itg\beta1^{-/-}$ MEFs and precipitated from extracts of three 15-cm dishes with GFP-Trap beads in the aforementioned lysis buffer. Lentivirally expressed GFP in $Itg\beta1^{-/-}$ MEFs served as a control for these precipitations. The precipitates were then analyzed for the presence of endogenous SNX17. SNX17 domains were cloned into pCherry-C1 (Takara Bio Inc.) according to domains listed in the UniProt database. The mCherry-tagged SNX17 constructs were then cotransfected into HEK293 cells with the GFP-tagged integrin cytoplasmic tail constructs and subjected to the same precipitation with anti-RFP beads (Chromotek) using the procedure and buffers described

for the GFP-Trap precipitations. For the in vitro translation, the mCherry-tagged FERM domain was subcloned into pCDNA3.1 to allow expression from the T7 promoter. The constructs were then in vitro translated with the coupled transcription/translation kit (TnT; Promega) according to the manufacturer's instructions. The translation mixes with the mCherry-tagged FERM domain were then mixed with equal volumes of the mixes with the GFP-tagged Itgβ1 tails, incubated for 10 min, diluted with 50 mM Tris, pH 7.8, and precipitated with GFP-Trap beads for 30 min. For the analysis of WASH complex association, GFP-tagged SNX17 and SNX27 were overexpressed in HEK293 cells, which were lysed in the aforementioned lysis buffer followed by GFP-Trap precipitation and analysis of endogenous WASH1, Strumpellin, and FAM21 antibody in the precipitates.

Image acquisition details

The fluorophores used in the study were anti–mouse amino-methyl-coumarin-acetate (Jackson ImmunoResearch Laboratories, Inc.), anti–rabbit Alexa Fluor 488 (Invitrogen), anti–mouse Alexa Fluor 594 (Invitrogen), and anti–goat Alexa Fluor 594 (Invitrogen). All samples were mounted in Mowiol mounting medium and imaged at room temperature. Microscopy images were taken on a confocal laser-scanning microscope (SP5 AOBS) attached to an inverted epifluorescence microscope (DMI6000). Camera and acquisition software used were the standard SP5 system software and camera. The objective used was a 63×, NA 1.4, oil immersion objective (Plan Apochromat BL). All images were subjected to removal of noise with Volocity using the standard remove noise function. For some images, brightness and contrast were increased uniformly over all images of the respective assay using Photoshop.

Online supplemental material

Fig. S1 shows quantification of SNX17 suppression by individual oligos and resultant effects on loss of Itgα5β1 as determined by SILAC-based proteomics, Western blot analysis, and a cell-based recycling assay. Fig. S2 shows quantitative colocalization of SNX17-GFP with endogenous EEA1 and LAMP1 and a time course of Itgβ1 internalization into and transport through early endosomes. Fig. S3 shows internalization of active versus inactive Itgβ1 into SNX17-GFP endosomes and the importance of the Y795A for retrieval from the lysosomal compartment. Video 1 shows the effects of SNX17 suppression on the migration of human fibroblasts in a cell-derived matrix. Online supplemental material is available at http://www.jcb.org/cgi/content/full/jcb.201111121/DC1.

The work was supported by the Swiss National Science Foundation, the Royal Society, and by the Wellcome Trust (grants 089928/Z/09/Z and 088419). M.D. Bass was supported by grant number 088419. We thank the Medical Research Council and Wolfson Foundation for supporting the Wolfson Bioimaging Facility at the University of Bristol.

Submitted: 25 November 2011
Accepted: 9 March 2012

References

Arighi, C.N., L.M. Hartnell, R.C. Aguilar, C.R. Haft, and J.S. Bonifacino. 2004. Role of the mammalian retromer in sorting of the cation-independent mannose 6-phosphate receptor. *J. Cell Biol.* 165:123–133. http://dx.doi.org/10.1083/jcb.200312055

Bass, M.D., R.C. Williamson, R.D. Nunan, J.D. Humphries, A. Byron, M.R. Morgan, P. Martin, and M.J. Humphries. 2011. A syndecan-4 hair trigger initiates wound healing through caveolin- and RhoG-regulated integrin endocytosis. *Dev. Cell*. 21:681–693. http://dx.doi.org/10.1016/j.devcel.2011.08.007

Burden, J.J., X.M. Sun, A.B. García, and A.K. Soutar. 2004. Sorting motifs in the intracellular domain of the low density lipoprotein receptor interact with a novel domain of sorting nexin-17. *J. Biol. Chem.* 279:16237–16245. http://dx.doi.org/10.1074/jbc.M313689200

Carlton, J., M. Bujny, B.J. Peter, V.M. Oorschot, A. Rutherford, H. Mellor, J. Klumperman, H.T. McMahon, and P.J. Cullen. 2004. Sorting nexin-1 mediates tubular endosome-to-TGN transport through coincidence sensing of high- curvature membranes and 3-phosphoinositides. *Curr. Biol.* 14:1791–1800. http://dx.doi.org/10.1016/j.cub.2004.09.077

Carlton, J., M. Bujny, A. Rutherford, and P.J. Cullen. 2005. Sorting nexins—unifying trends and new perspectives. *Traffic*. 6:75–82. http://dx.doi.org/10.1111/j.1600-0854.2005.00260.x

Caswell, P.T., S. Vadrevu, and J.C. Norman. 2009. Integrins: masters and slaves of endocytic transport. *Nat. Rev. Mol. Cell Biol.* 10:843–853. http://dx.doi.org/10.1038/nrm2799

Cullen, P.J. 2008. Endosomal sorting and signalling: an emerging role for sorting nexins. *Nat. Rev. Mol. Cell Biol.* 9:574–582. http://dx.doi.org/10.1038/nrm2427

Cullen, P.J., and H.C. Korswagen. 2012. Sorting nexins provide diversity for retromer-dependent trafficking events. *Nat. Cell Biol.* 14:29–37. http://dx.doi.org/10.1038/ncb2374

Dozynkiewicz, M.A., N.B. Jamieson, I. Macpherson, J. Grindlay, P.V. van den Berghe, A. von Thun, J.P. Morton, C. Gourley, P. Timpson, C. Nixon, et al. 2012. Rab25 and CLIC3 collaborate to promote integrin recycling from late endosomes/lysosomes and drive cancer progression. *Dev. Cell*. 22:131–145. http://dx.doi.org/10.1016/j.devcel.2011.11.008

Ghai, R., M. Mobli, S.J. Norwood, A. Bugarcic, R.D. Teasdale, G.F. King, and B.M. Collins. 2011. Phox homology band 4.1/ezrin/radixin/moesin-like proteins function as molecular scaffolds that interact with cargo receptors and Ras GTPases. *Proc. Natl. Acad. Sci. USA*. 108:7763–7768. http://dx.doi.org/10.1073/pnas.1017110108

Gomez, T.S., and D.D. Billadeau. 2009. A FAM21-containing WASH complex regulates retromer-dependent sorting. *Dev. Cell*. 17:699–711. http://dx.doi.org/10.1016/j.devcel.2009.09.009

Grant, B.D., and J.G. Donaldson. 2009. Pathways and mechanisms of endocytic recycling. *Nat. Rev. Mol. Cell Biol.* 10:597–608. http://dx.doi.org/10.1038/nrm2755

Harterink, M., F. Port, M.J. Lorenowicz, I.J. McGough, M. Silhankova, M.C. Betist, J.R. van Weering, R.G. van Heesbeen, T.C. Middelkoop, K. Basler, et al. 2011. A SNX3-dependent retromer pathway mediates retrograde transport of the Wnt sorting receptor Wntless and is required for Wnt secretion. *Nat. Cell Biol.* 13:914–923. http://dx.doi.org/10.1038/ncb2281

Huss, M., and H. Wieczorek. 2009. Inhibitors of V-ATPases: old and new players. *J. Exp. Biol.* 212:341–346. http://dx.doi.org/10.1242/jeb.024067

Johannes, L., and V. Popoff. 2008. Tracing the retrograde route in protein trafficking. *Cell*. 135:1175–1187. http://dx.doi.org/10.1016/j.cell.2008.12.009

Jović, M., N. Naslavsky, D. Rapaport, M. Horowitz, and S. Caplan. 2007. EHD1 regulates beta1 integrin endosomal transport: effects on focal adhesions, cell spreading and migration. *J. Cell Sci.* 120:802–814. http://dx.doi.org/10.1242/jcs.03383

Lane, R.F., S.M. Raines, J.W. Steele, M.E. Ehrlich, J.A. Lah, S.A. Small, R.E. Tanzi, A.D. Attie, and S. Gandy. 2010. Diabetes-associated SorCS1 regulates Alzheimer's amyloid-beta metabolism: evidence for involvement of SorL1 and the retromer complex. *J. Neurosci.* 30:13110–13115. http://dx.doi.org/10.1523/JNEUROSCI.3872-10.2010

Lauffer, B.E., C. Melero, P. Temkin, C. Lei, W. Hong, T. Kortemme, and M. von Zastrow. 2010. SNX27 mediates PDZ-directed sorting from endosomes to the plasma membrane. *J. Cell Biol.* 190:565–574. http://dx.doi.org/10.1083/jcb.201004060

Lee, J., C. Retamal, L. Cuitiño, A. Caruano-Yzermans, J.E. Shin, P. van Kerkhof, M.P. Marzolo, and G. Bu. 2008. Adaptor protein sorting nexin 17 regulates amyloid precursor protein trafficking and processing in the early endosomes. *J. Biol. Chem.* 283:11501–11508. http://dx.doi.org/10.1074/jbc.M800642200

Li, J., B.A. Ballif, A.M. Powelka, J. Dai, S.P. Gygi, and V.W. Hsu. 2005. Phosphorylation of ACAP1 by Akt regulates the stimulation-dependent recycling of integrin beta1 to control cell migration. *Dev. Cell*. 9:663–673. http://dx.doi.org/10.1016/j.devcel.2005.09.012

Lobert, V.H., A. Brech, N.M. Pedersen, J. Wesche, A. Oppelt, L. Malerød, and H. Stenmark. 2010. Ubiquitination of alpha 5 beta 1 integrin controls fibroblast migration through lysosomal degradation of fibronectin-integrin complexes. *Dev. Cell*. 19:148–159. http://dx.doi.org/10.1016/j.devcel.2010.06.010

Margadant, C., H.N. Monsuur, J.C. Norman, and A. Sonnenberg. 2011. Mechanisms of integrin activation and trafficking. *Curr. Opin. Cell Biol.* 23:607–614. http://dx.doi.org/10.1016/j.ceb.2011.08.005

Moser, M., K.R. Legate, R. Zent, and R. Fässler. 2009. The tail of integrins, talin, and kindlins. *Science*. 324:895–899. http://dx.doi.org/10.1126/science.1163865

Muhammad, A., I. Flores, H. Zhang, R. Yu, A. Staniszewski, E. Planel, M. Herman, L. Ho, R. Kreber, L.S. Honig, et al. 2008. Retromer deficiency observed in Alzheimer's disease causes hippocampal dysfunction, neurodegeneration, and Abeta accumulation. *Proc. Natl. Acad. Sci. USA*. 105:7327–7332. http://dx.doi.org/10.1073/pnas.0802545105

Roca-Cusachs, P., N.C. Gauthier, A. Del Rio, and M.P. Sheetz. 2009. Clustering of α(5)β(1) integrins determines adhesion strength whereas α(v)β(3) and talin enable mechanotransduction. *Proc. Natl. Acad. Sci. USA*. 106:16245–16250. http://dx.doi.org/10.1073/pnas.0902818106

Salicioni, A.M., A. Gaultier, C. Brownlee, M.K. Cheezum, and S.L. Gonias. 2004. Low density lipoprotein receptor-related protein-1 promotes beta1

integrin maturation and transport to the cell surface. *J. Biol. Chem.* 279:10005–10012. http://dx.doi.org/10.1074/jbc.M306625200

Seaman, M.N. 2004. Cargo-selective endosomal sorting for retrieval to the Golgi requires retromer. *J. Cell Biol.* 165:111–122. http://dx.doi.org/10.1083/jcb.200312034

Seet, L.F., and W. Hong. 2006. The Phox (PX) domain proteins and membrane traffic. *Biochim. Biophys. Acta*. 1761:878–896.

Stockinger, W., B. Sailler, V. Strasser, B. Recheis, D. Fasching, L. Kahr, W.J. Schneider, and J. Nimpf. 2002. The PX-domain protein SNX17 interacts with members of the LDL receptor family and modulates endocytosis of the LDL receptor. *EMBO J.* 21:4259–4267. http://dx.doi.org/10.1093/emboj/cdf435

Temkin, P., B. Lauffer, S. Jäger, P. Cimermancic, N.J. Krogan, and M. von Zastrow. 2011. SNX27 mediates retromer tubule entry and endosome-to-plasma membrane trafficking of signalling receptors. *Nat. Cell Biol.* 13:715–721. http://dx.doi.org/10.1038/ncb2252

Tiwari, A., J.J. Jung, S.M. Inamdar, C.O. Brown, A. Goel, and A. Choudhury. 2011. Endothelial cell migration on fibronectin is regulated by syntaxin 6-mediated alpha5beta1 integrin recycling. *J. Biol. Chem.* 286:36749–36761. http://dx.doi.org/10.1074/jbc.M111.260828

van Kerkhof, P., J. Lee, L. McCormick, E. Tetrault, W. Lu, M. Schoenfish, V. Oorschot, G.J. Strous, J. Klumperman, and G. Bu. 2005. Sorting nexin 17 facilitates LRP recycling in the early endosome. *EMBO J.* 24:2851–2861. http://dx.doi.org/10.1038/sj.emboj.7600756

Wassmer, T., N. Attar, M.V. Bujny, J. Oakley, C.J. Traer, and P.J. Cullen. 2007. A loss-of-function screen reveals SNX5 and SNX6 as potential components of the mammalian retromer. *J. Cell Sci.* 120:45–54. http://dx.doi.org/10.1242/jcs.03302

Wassmer, T., N. Attar, M. Harterink, J.R. van Weering, C.J. Traer, J. Oakley, B. Goud, D.J. Stephens, P. Verkade, H.C. Korswagen, and P.J. Cullen. 2009. The retromer coat complex coordinates endosomal sorting and dynein-mediated transport, with carrier recognition by the trans-Golgi network. *Dev. Cell*. 17:110–122. http://dx.doi.org/10.1016/j.devcel.2009.04.016

White, D.P., P.T. Caswell, and J.C. Norman. 2007. αvβ3 and α5β1 integrin recycling pathways dictate downstream Rho kinase signaling to regulate persistent cell migration. *J. Cell Biol.* 177:515–525. http://dx.doi.org/10.1083/jcb.200609004

Worby, C.A., and J.E. Dixon. 2002. Sorting out the cellular functions of sorting nexins. *Nat. Rev. Mol. Cell Biol.* 3:919–931. http://dx.doi.org/10.1038/nrm974

Zech, T., S.D. Calaminus, P. Caswell, H.J. Spence, M. Carnell, R.H. Insall, J. Norman, and L.M. Machesky. 2011. The Arp2/3 activator WASH regulates α5β1-integrin-mediated invasive migration. *J. Cell Sci.* 124:3753–3759. http://dx.doi.org/10.1242/jcs.080986